6

Library L-M-A-L.

~~4573~~

TECHNICAL MEMORANDUMS

NATIONAL ADVISORY COMMITTEE FOR AERONAUTICS

No. 821

ON THE ACTUAL LOADS ON AIRPLANE LANDING GEARS

By S. Shiskin

Central Aero-Hydrodynamical Institute

4, 7, 7

Washington
March 1937

NATIONAL ADVISORY COMMITTEE FOR AERONAUTICS

TECHNICAL MEMORANDUM NO. 821

ON THE ACTUAL LOADS ON AIRPLANE LANDING GEARS*

By S. Shiskin

I. INTRODUCTION

The problem of the actual loads exerted on the airplane landing gear has long engaged the attention of the airplane designer. Repeated tests have been conducted for the purpose of determining the forces acting on the landing wheels during landing. Two methods have been applied to the solution of this problem, one of which was to measure the accelerations by means of an accelerometer, the other to measure the displacements of the shock-absorber systems. The first method has the serious disadvantage that the readings of the accelerometer strongly depend on the location and method of attachment of the accelerometer to the airplane and it always remains unclear just what mass is to be taken in connection with the accelerometer reading in computing the force from the acceleration. By the second method only the maximum travel of the shock absorber in the landing and take-off runs is measured. This latter method is of little use in determining the force with a rubber-cord shock absorber since the properties of rubber depend very much on the temperature and the rate at which the load is applied. The error from the last cause alone may amount to more than 20 percent. For an oleo-shock-absorption mechanism the actual form of the dependence of the shock-absorber force on the piston travel is even more uncertain since the laboratory tests with such apparatus are few in number.

The methods described above give no indication of the direction of the force acting on the wheel and are intended to give only a rough approximation of this force. It has now been found possible to obtain a considerably more accurate solution of this problem as a result of the application of an apparatus, developed in the flight tests of the Central Aerodynamical Institute (CAHI), for obtaining a time-history record of the stresses in the chassis members by means of extensometer measurements.

---

*Report No. 269, of the Central Aero-Hydrodynamical Institute, Moscow, 1936.

II. PROCEDURE

Extensometers were placed on all important members of the landing gear, their readings being synchronized by time recorders. Readings were first recorded on all instruments with the airplane at rest. The airplane was then allowed to take off and another record obtained with the airplane flying level and smoothly at low velocities. With the aid of these recordings it was possible to determine the stresses in each landing-gear member with the airplane at rest. After this the regular take-off and landing runs were made. Knowing the stress history of all the important elements of the landing gear during the various runs, it is a simple matter to compute the forces and their resultant acting on the landing-gear wheel. The resultant will be obtained both in magnitude and direction. The data thus obtained supply the designer with information on the actual forces exerted on the landing-gear members and the load factors.

As an illustration and check, the external force P acting on the airplane wheel at rest was determined by the above method. For airplane no. 1 the force was thus found to be P = 1,872 kilograms as compared with the known value, 1,900 kilograms.

III. OBJECT OF INVESTIGATION

The investigation was intended to throw light on a number of problems:

1. Obtain a time history of the force acting on the gear wheels during the take-off and landing runs.

2. Obtain the time history of the direction of this force (magnitude of its three components along the coordinate axes).

3. Derive conclusions as to the design load factors.

In connection with the latter, of especial interest was the solution of such problems as: (a) the dynamic loads in the three main landing attitudes, namely, a 3-point landing, horizontal load landing, and landing with side load; (b) the problem of the true direction of the forces for each of the above "pure" types of landing; (c) combination of the above types; and (d) the comparison for each of the chassis members of the computed force (according to the design standards) with the actual force measured in the tests so as to determine the actual factors of safety.

IV. RESULTS

The landing gears of two airplanes were investigated in the take-off and landing runs. The landing gear of no. 1 airplane is of especial interest, being of modern construction with pneumatic-oleo-shock absorbers and 900 by 200 pneumatic tires. Landing gear no. 2 was provided with a rubber-disk shock-absorbing mechanism and 900 by 200 tires. It is also proposed in the near future to carry out tests on the same airplanes provided with skis. We shall now consider the data for each of the landing gears.

1. Landing Gear No. 1

A. Landing-gear structure.- A sketch of the landing-gear arrangement is shown on figure 1. As seen from the figure, the landing gear may be considered to be a combination of the column 2-5 with a very simple girder. Points 3, 3', and 4 may be considered as rigid supports. Point 2 may be considered as a rigid support in plane XZ and a roller support in the direction of the Y axis, since it is connected to the longeron where there are no struts attached. The axial force on the member 2-5 is therefore eventually taken up not by support 2 but by supports 3 and 3' through the medium of struts 0-3 and 0-3'.

The above arrangement of the landing-gear members is very convenient for the purposes of our investigation and makes possible a simple and reliable determination of the magnitude of the components of the force P acting on the wheel by measuring the forces in each of the struts. Thus, the projection on the X axis of the force on member 1-4, corrected for the lever arm of the member 1-2, immediately gives the horizontal component P_x, i.e.,

$$P_x = (S_{1-4})_x \frac{l_{1-2}}{l_{2-5}} = 0.484\ (S_{1-4})_x$$

Similarly, the sum of the projections on the Z axis of the forces on members 0-3 and 0-3' (with lever arm correction) gives the side component P_z:

$$\left[(S_{0-3})_z + (S_{0-3'})_z\right] \frac{l_{0-2}}{l_{2-6}} = 0.455 \left[(S_{0-3})_z + (S_{0-3'})_z\right]$$

The sum of the projections on the Y axis of the forces on the three struts: 0-3, 0-3', and 1-4, is directly equal to P_y. It should be observed that the struts are hinged at each end, the hinges having each a single axis of rotation. The extensometers were placed on the struts as shown in figure 2, so as to exclude the effect of possible secondary bending stresses. The portion 1-2 of strut 2-5 was not investigated with extensometers, since it consisted of a shock-absorbing cylinder so that the stress at any point depended on the piston position. In general, the stresses in this portion were of little interest since they could not be large due to the small rigidity of support 2 with respect to the Y axis.

B. Computed data for no. 1 landing gear.- We shall now consider the results obtained for the no. 1 landing gear. The computed data consist of: (1) a time history of the external force P acting on the wheel, curves of its components P_x, P_y, and P_z (see figs. 3-9); and (2) tables of the forces on the members and the computed components of the force P. The tables are given in part in the text (see table I) and are fully presented in appendix I. The parts of the tables given in the text are taken for the instants of time giving the maximum overloads and forces, the values of which were used farther on.

C. Analysis of computed data.- The strength standards for the landing gear tend to be based on the three conditions of landing described above, namely, where the force is vertical (E), horizontal (G), and side (F). We shall therefore consider the maximum load factors for each of these cases: vertical (E), forward (G), and side (F) with the object of comparing the experimental values with those obtained by the standard computations.

TABLE I

Landing 1, Airplane No. 1

	0-3'	0-3	1-4	Impact no. 1; t=0 sec.		
				Σ	KΣ	P (kg)
S ...	-1946	-4100	+1740			
S_x ...	0	0	+1418	+1418	$\boxed{+686}$	
S_y ...	-1751	-3690	+1005	-4436	$\boxed{-4436}$	4509
S_z ...	-848	+1788	0	+940	+428	
S ...	-1845	$\boxed{-4200}$	+2020	Impact no. 2; t=1.5 sec.		
S_x ...	0	0	+1646	+1646	$\boxed{+796}$	
S_y ...	-1661	-3780	+1167	-4274	$\boxed{-4274}$	4372
S_z ...	-804	+1831	0	+1027	+467	
S ...	-1230	-2151	$\boxed{+2680}$	Impact no. 22; t=17.5 sec.		
S_x ...	0	0	+2184	+2184	+1056	
S_y ...	-1107	-1936	+1549	-1494	-1494	1839
S_z ...	-536	+937	0	+401	+182	

Landing 2, Airplane No. 1

S ...	-2563	-3075	$\boxed{-1608}$	Impact no. 4; t=3.7 sec.		
S_x ...	0	0	-1310	-1310	$\boxed{-634}$	
S_y ...	-2307	-2768	-929	-6004	$\boxed{-6004}$	6038
S_z ...	-1117	+1341	0	+224	+102	
S ...	-2040	$\boxed{+2050}$	-668	Impact no. 5; t=5.3 sec.		
S_x ...	0	0	-545	-545	-264	
S_y ...	-1842	+1845	-387	-384	-384	940
S_z ...	-893	-894	0	-1787	$\boxed{-815}$	

Landing 3, Airplane No. 1

S ...	-1230	+1640	-1338	Impact no. 8; t=8.58 sec.		
S_x ...	0	0	-1090	-1090	-527	
S_y ...	-1105	+1475	-774	-404	-404	873
S_z ...	-536	-714	0	-1250	-567	
S ...	-1640	-3075	-1606	Impact no. 12; t=12 sec.		
S_x ...	0	0	-1310	-1310	$\boxed{-634}$	
S_y ...	-1480	-2775	-928	-5183	-5183	5229
S_z ...	-715	+1340	0	+625	+285	

The largest value for the vertical load factor was obtained for the landing of no. 2 landing gear 4 seconds after the first impact with the ground, the value being

$$\eta_{y_{max}} = \frac{P_y}{P_{y^o}} = \frac{P_y}{P_o \cos \gamma}$$

where P_o is the pressure on the wheel when at rest and γ is the ground angle, i.e.,

$$\eta_{y_{max}} = \frac{6004}{1900 \cos 13^o} = 3.24$$

(The design load factor for this landing gear was 4.5.) It is proper to remark here that high values of P_y are obtained, as a rule, not at the instant of first contact with the ground but later in the landing run, and the loads during the take-off run are near and sometimes even exceed those during the landing run.

The maximum value of the side load factor $\eta_{z_{max}}$ was obtained during the landing of no. 2, 6 seconds after first impact, the force acting in the direction from wheel toward the plane of symmetry of the airplane:

$$\eta_{z_{max}} = \frac{815}{G/2} = \frac{815}{2125} = 0.383 \quad \text{(computed value 1.1)}$$

Here G denotes the weight of the airplane during the test.

The value of $\eta_{x_{max}}$ (opposite to the flight direction) was likewise obtained during the second and third landings after 4, and 12 seconds, respectively:

$$\eta_{x_{max}} = \frac{P_x}{\frac{G}{2} \cos (\gamma + 20^o)} = \frac{634}{1780} = 0.356 \quad \text{(computed value 3)}$$

Comparison of the actual and standardized load factors does not determine, however, the values of the safety factors since in practice all the three components act simultaneously on the fuselage members. The safety factors must therefore be considered with respect to the maximum forces in the struts as computed and as obtained from experiment.

TABLE II

Name of member	Notation	Computed maximum load P	Experimental maximum load P	P_{exp}/P_{comp}
Wheel strut	1-5	-8,320 (E)	-6,004	1.39
Side struts	0-3 0-3'	±5,900 (F)	-4,200 +2,050	1.4
Rear strut	1-4	-13,400 (G) +4,900	-1,608	8.35*

*See section V.

The strut 1-5 is of lower strength than that assumed by the design norms since the maximum computed safe load factor was determined as equal to 3 in the damping computations, and in the rough landing of no. 2 the value of 3.24 was reached. The side struts have a lower strength for the reason that, as may be seen from table I, the severest case of vertical load was accompanied by side impact.

Let us now consider the question of the direction of the force P and the comparison with that assumed in the design norms.

D. Various conditions of landing on landing gear no. 1.- (a) Three-point landing, Case E: According to the norms, the force P_E is inclined forward of the vertical by angle β equal to the landing angle γ. In considering this case it is particularly interesting to note a considerable vertical component of the force P_E and the fact that the horizontal component is in the flight direction. Let us see what the direction of the force P_x actually is.

For $P_{y_{max}} = 6,004$ kg (landing 2, 4 seconds) the direction of the horizontal component P_x is opposite to that assumed in the standards, since to case E there is here added the horizontal impact of the maximum force during the test. For other instants and at other landings we find the force P_E inclined in a forward direction at considerable values of P_y (table III).

TABLE III

Landing	Seconds	P_y	P_x (against flight direction)	Angle β
Landing no. 1	3.5	5,431	-634	6° 40'
Landing no. 1	0	4,436	-686	8° 50'
Landing no. 1	1.5	4,274	-796	10° 30'

The force P_E may thus have a direction approaching near that of the norms.

(b) Case G, forward impact: According to the norms, the force P_G lies in the plane X-Y and is inclined to the horizontal by the angle $\gamma + 20^\circ$, i.e., in the given case by 33° (figs. 10 and 11). At the instant when P_x has its maximum value and is equal to 634 kilograms (i.e., at the fourth and twelfth second of the second and third landings), there is also a component P_y equal, respectively, to 6,004 kilograms (likewise a maximum) and 5,183 kilograms and the side component P_z is at 35 percent of its maximum value. It therefore follows that a considerable vertical component may be present at the horizontal impact. The angle β, at $P_{y_{max}} = 6,004$ kg and $P_x =$ 634 kg, will be

$$\beta = \gamma + 70^\circ$$

From the tests it is evident, however, that the angle β may have very different values and in general may be near the normalized value. Thus, for landing no. 3, after 8.58 seconds, it is equal to $\gamma + 24.5^\circ$ (with $P_y = 404$ kg and $P_x = 527$ kg). The vertical component in this case is small and the horizontal component is 83 percent of its maximum value.

(c) Case F, side impact: According to the norms, the force P_F acts at the rim of the wheel in the direction of the Z axis. The test indicates the actual existence of such a force and that it may be directed from the wheel toward the axis of symmetry as well as in the opposite direction. The maximum values of P_z are: toward the axis of symmetry, +815 kg (landing 2, impact 5); toward the wing tip, 467 kg (landing 1, impact 2). At the instant when P_z is at its maximum value and is equal to 815 kilograms, i.e., after 6 seconds of the second landing, there is also a horizontal thrust of amount 264 kilograms, equal to 42 percent of the maximum, and a small vertical component P_y equal to 387 kilograms. In general, in cases of considerable side impact (near 50 percent of the maximum value and above), the vertical component sometimes assumes a large value up to as much as 74 percent. For example, landing 1, 0 second, P_z = 428 kg (52 percent), P_y = 4,436 kg (74 percent).

As an illustration of what has been said above on the simultaneous action of the different types of loads, there is presented in figure 12 a time history of the forces acting on the landing gear in the XY and ZY planes. As may be seen from the figure, the airplane first rested on the wheel and ran a few seconds under the action of a forward thrust, the tail was then let down, the direction of the force being the usual one for a 3-point landing, and then the landing gear again experienced a force in the horizontal direction. During the entire landing and landing run there were side loads acting mostly in the direction from wheel toward the axis of symmetry of the airplane.

2. Landing Gear of Airplane No. 2

<u>A. The arrangement of this landing gear is shown on figure 13.</u>

<u>B. Computed data</u>.- The extensometers were placed on all the fuselage struts of one-half the landing gear. For this landing gear we shall analyze only the P_y and P_x components. The results are presented partially in table IV and figures 14-17, and are given fully in appendix 2.

TABLE IV

	1-2	1-3	4-2	4-2'	Σ	P
			Landing 1, Airplane No. 2			
S ...	-2450	$\boxed{-1182}$	+1580	-920	Impact no. 11; t=8.6	
S_x ...	431	-923	-	-	-492	+492
S_y ...	-2100	-	-	-	-2100	1772
			Landing 2, Airplane No. 2			
S ...	-1225	-788	$\boxed{-2235}$	-1050	Impact no. 6; t=3.5	
S_x ...	+216	-615	-	-	-399	+399
S_y ...	-1050	-	-	-	-1050	+885
S ...	-3430	+394	+1050	+1445	Impact no. 18; t=9.6	
S_x ...	+604	+307	-	-	+911	$\boxed{-911}$
S_y ...	-2940	-	-	-	-2940	$\boxed{+2480}$
S ...	$\boxed{-3680}$	-335	+920	+1445	Impact no. 20; t=10.7	
S_x ...	+647	-262	-	-	+385	$\boxed{-385}$
S_y ...	-3154	-	-	-	-3154	$\boxed{+2659}$
			Take-off 1, Airplane No. 2			
S ...	-735	-920	1970	2365	Impact no. 11; t=5.7	
S_x ...	130	-718	-	-	-588	$\boxed{+588}$
S_y ...	-630	-	-	-	-630	$\boxed{+531}$

C. Discussion of results.- The maximum value of the vertical load factor was obtained for landing no. 2, impact no. 20. The value is

$$\eta_{y_{max}} = \frac{2659}{1330 \cos 12^\circ} = 2.05 \quad \text{(computed value about 6)}$$

Here the value 1,330 kilograms denotes the pressure on the wheel of the airplane at rest, and 12° is the ground angle of the airplane.

The maximum value of η_x is obtained for flight 1, impact no. 11:

$$\eta_{x_{max}} = \frac{588}{\frac{2995}{2} \cos 32^\circ} = 0.464 \quad \text{(value computed according to norms is 3)}$$

Here 2,995 kilograms is the weight of the airplane during the test and 32° is the ground angle of the airplane +20° according to the norms.

Table V gives the factors of safety for the various landing-gear struts.

TABLE V

Member	P computed	P experimental maximum	$f = \frac{P_{comp}}{P_{exp}}$
1-2	-11,000	-3,680	2.99
1-3 2-4	-5,000	-1,182	4.23
2'-4	-2,930 (F)	-2,235	1.31

D. Discussion of the different types of landing on landing gear no. 2.

(a) Case E: At the value $P_{y_{max}} = 2,659$ kg the direction of the horizontal component P_x agrees with the standard (landing 2, impact 20). The angle the force makes with the vertical plane is

$$\beta = \text{arc tan} \frac{385}{2659} = 8^\circ\ 15' \quad (12^\circ \text{ according to norms})$$

This angle has a larger value at somewhat smaller values of P_y. Thus, for the same second landing, impact no. 18,

$$\beta = \text{arc tan} \frac{911}{2480} \cong 20^\circ \quad (\text{i.e., even exceeds the norms somewhat})$$

(b) Case G: At the instant when P_x has its maximum in the forward direction equal to 588 kilograms, there is a vertical component $P_y = 531$ kg. Thus, the angle the direction of P_G makes with the XZ plane will be

$$\beta = \text{arc tan} \frac{531}{588} = 42^\circ$$

while, according to the norms, it is 20° + 12° = 32°. Thus, the actual direction of the force P_G is near that of the norms, although for a somewhat smaller forward force. On figure 18 is shown graphically the time history of the force acting on the wheel in the plane XY during flight 1.

V. SUMMARY OF RESULTS AND CONCLUSIONS

In tables VI and VII are brought together the results obtained in section 4 on both landing gears. The first table (table VI) gives the comparison of the values of the "maximum applied" loads assumed by the norms (i.e., the maximum break-down loads divided by the safety factor 1.5) with the maximum loads obtained in the tests, and there is also given the ratio between them for each of the landing-gear members. In the second table (table VII) are brought together the results of the investigation on the simultaneous action of the different standardized types of landing impact as obtained for landing gear no. 1.

TABLE VI

Landing gear	Maximum computed / Maximum experimental			Member	P_{comp}	Maximum P_{exp}	$\frac{P_{comp}}{P_{exp}}$	
	η_y	η_x	η_z					
1	$\frac{3}{3.24}$	$\frac{2}{0.356}$	$\frac{0.734}{0.383}$	1-5	-8,320	-6,004	1.39	Pneumatic-oleo shock absorber 900 by 200 air wheels, split axle
				0-3 0-3'	±5,900	-4,200 +2,050	1.4	
				1-4	-13,400 +4,900	-1,608 +2,680	8.35	
2	$\frac{4.0}{2.05}$	$\frac{2}{0.464}$	-	1-2	-11,000	-3,680	2.99	Rubber disk shock absorber 900 by 200 air wheels, continuous axle
				1-3	-5,000	-1,182	4.23	
				2-4 2'-4	-2,930	-2,235	1.31	

TABLE VII

Landing Gear No. 1

Landing	Percent of maximum test value (1)			Percent of maximum value according to norms (2)			Notes
	P_y	P_x	P_z	P_y	P_x	P_z	
2 landing, 4 seconds	100	100	12.5	108	18	6.5	(1) Maximum values from test: P_y = 6,004 kg
3 landing, 12 seconds	86.5	100	35	93.5	18	18.3	P_x = 634 kg P_z = 815 kg
2 landing, 6 seconds	6.5	42	100	7	7.5	52	(2) Maximum values according to norms:
1 landing, 0 second	74.0	-	52	80	-	27	P_y = 8320/1.5=5550 P_x = 5350/1.5=3560
1 landing, 1.5 seconds	71.3	-	57.3	77	-	30	P_z = 2340/1.5=1560

From an examination of tables VI and VII, as well as the preceding data, the following conclusions may be derived:

1. Case E (vertical impact): A 3-point landing may actually take place as assumed, such that the conventional direction of the force (normal to the ground in the static position of the airplane) is maintained throughout. As far as the magnitude of the force is concerned, it should be observed that, in general, it agrees well with the assumed norms, although a case occurred for which the computed force was exceeded (η_y = 3.24 instead of 3), and this in our opinion may be explained not by any defect in the shock absorber but by a certain disagreement between the computed and actual forces. This condition may be corrected only by increasing the factor of safety from 1.5 to 1.6-1.8, i.e., causing this factor to approach more nearly the value customary for structures operating under bending stresses.

2. Case G (horizontal impact): Actually occurs as far as the direction of the force is concerned, but the force is by far not as great as that assumed in the norms (instead

of the assumed load factor $\frac{3}{1.5} = 2$, the maximum obtained was 0.464).

In the case of landing gear no. 1, there was a striking difference between the computed and actual force obtained for the rear strut (1,608 instead of 12,000 to 13,000), in spite of the fact that the landings were sudden with the vertical load attaining its maximum. It should be borne in mind, of course, that the landings were made on a good landing field, but still it is clear that the load factor for this case may be lowered. The design standards of other countries do not give such a large value for the horizontal force as do our standards, their value being about one-third as large but with the vertical component being larger as a rule. A sufficiently cautious figure for the load factor would be $\eta_G = 2$. However, in addition to this simple case G, the additional case of the simultaneous action of types E and G must be considered. It would be most expedient to assume the force in the XY plane, applied at the center of gravity of the airplane. For the usual ground angle of about 12° to 14° we then obtain, for a "typical" value $\eta_E = 5$, the value $\eta_G = 5 \sin (12^\circ - 14^\circ) \cong 1$.

3. Case F (side impact): Does not take place as assumed in the design standards as there is always the accompanying action of case E. The load factor of our standards $\eta_F = \frac{V_{landing}}{100}$ appears to be a safe value and this is confirmed both by experiment and by comparison with the foreign standards where the value of η_F varies between 0.5 and 1. The several failures of the landing gear in landing in a side wind that have occurred recently are explained for the most part by the simultaneous action of a considerable vertical component which, as a rule, is very unfavorable to the structure with the present-day split-axle type of landing gear. For the above reason we propose that the "pure" case F be entirely removed as a separate case in the design rules and be considered only in connection with case E acting simultaneously, the load factor η_F being defined by the preceding formula. As far as η_E is concerned, for this new mixed case, our test did not give any coincidence in the maxima of the vertical and side components. The worst condition occurred for a value P_y = 75 percent of $P_{y_{max}}$ when P_z = 60 percent of $P_{z_{max}}$. In the light of the recent accidents,

however, and taking into account the peculiarities of modern chassis design (split-axle type), we should assume a complete combination (100 percent) of cases E and F as correct. The introduction of this new case removes the necessity of any special consideration of landings in a side wind.

Translation by S. Reiss,
National Advisory Committee
for Aeronautics.

Appendix I

Forces on landing gear members, their components and the resultants acting on the wheel.

Landing No. 1, Airplane No. 1

	0–3'	0–3	1–4	Σ	kΣ	P
				Impact No. 1; t = 0 sec.		
S	−1946	−4100	+1740	Σ	kΣ	P
S_x	0	0	+1418	+1418	+ 686	
S_y	−1751	−3690	+1005	−4436	−4436	4509
S_z	− 848	+1788	0	+ 940	+ 428	
				Impact No. 2; t = 1.5 sec.		
S	−1845	−4200	+2020			
S_x	0	0	+1646	+1646	+ 796	
S_y	−1661	−3780	+1167	−4274	−4274	4372
S_z	− 804	+1831	0	+1027	+ 467	
				Impact No. 3; t = 3.5 sec.		
S	−3585	−3481	+1608			
S_x	0	0	+1310	+1310	+ 634	
S_y	−3226	−3133	+ 928	−5431	−5431	5468
S_z	−1563	+1518	0	− 45	− 24	
				Impact No. 4; t = 4.7 sec.		
S	−3075	−1947	+ 936			
S_x	0	0	+ 762	+ 762	+ 369	
S_y	−2767	−1752	+ 541	−3978	−3978	4013
S_z	−1341	+ 848	0	− 493	− 224	
				Impact No. 5; t = 6 sec.		
S	−2560	−1334	+1876			
S_x	0	0	+1529	+1529	+ 740	
S_y	−2304	−1201	+1084	−2421	−2421	2543
S_z	−1116	+ 581	0	− 535	− 243	
				Impact No. 6; t = 6.7 sec.		
S	−2150	−1127	+1876			
S_x	0	0	+1529	+1529	+ 740	
S_y	−1935	−1014	+1084	−1865	−1865	2017
S_z	− 937	+ 491	0	− 446	− 203	
				Impact No. 7; t = 7.35 sec.		
S	−1947	−1538	+1204			
S_x	0	0	+ 981	+ 981	+ 475	
S_y	−1752	−1384	+ 695	−2441	−2441	2488
S_z	− 848	+ 670	0	− 178	− 81	
				Impact No. 8; t = 8 sec.		
S	−1640	−1947	+ 668			
S_x	0	0	+ 544	+ 544	263	
S_y	−1476	−1752	+ 386	−2842	−2842	2354
S_z	− 715	+ 848	0	+ 133	+ 61	
				Impact No. 9; t = 8.5 sec.		
S	−1314	−2050	+ 668			
S_x	0	0	+ 544	+ 544	+ 263	
S_y	−1201	−1845	+ 386	−2680	−2680	2697
S_z	− 582	+ 894	0	+ 312	+ 141	
				Impact No. 10; t = 0 sec.		
S	−1640	−1947	+ 668			
S_x	0'	0	+ 544	+ 544	+ 263	
S_y	−1476	−1752	+ 386	−2842	−2842	2854
S_z	− 715	+ 848	0	+ 133	+ 61	
				Impact No. 11; t = 10 sec.		
S	−1538	−2255	+1204			
S_x	0	0	+ 981	+ 981	+ 475	
S_y	−1384	−2030	+ 695	−2719	−2719	2764
S_z	− 670	+ 983	0	+ 313	+ 142	
				Impact No. 12; t = 10.5 sec.		
S	−2560	−3172	+1338			
S_x	0	0	+1090	+1090	+ 527	
S_y	−2304	−2855	+ 773	−4386	−4386	4419
S_z	−1116	+1383	0	+ 267	+ 122	
				Impact No. 13; t = 11.15 sec.		
S	−2050	−2354	+1740			
S_x	0	0	+1418	+1418	+ 686	
S_y	−1845	−2119	+1005	−2959	−2959	3038
S_z	− 894	+1026	0	+ 132	+ 60	
				Impact No. 14; t = 11.75 sec.		
S	−1845	−2050	+1740			
S_x	0	0	+1418	+1418	+ 686	
S_y	−1661	−1845	+1005	−2501	−2501	2594
S_z	− 804	+ 894	0	+ 90	+ 41	
				Impact No. 15; t = 12.45 sec.		
S	−1435	−1538	+ 936			
S_x	0	0	+ 762	+ 762	+ 369	
S_y	−1291	−1384	+ 541	−2134	−2134	2166
S_z	− 625	+ 670	0	+ 45	+ 20	
				Impact No. 16; t = 13.25 sec.		
S	−1435	−1538	+1072			
S_x	0	0	+ 874	+ 874	+ 423	
S_y	−1291	−1384	+ 619	−2056	−2056	2099
S_z	− 525	+ 670	0	+ 45	+ 20	
				Impact No. 17; t = 13.9 sec.		
S	−1640	−2563	1876			
S_x	0	0	+1529	+1529	+ 740	
S_y	−1476	−2307	+1084	−2699	−2699	2804
S_z	− 715	+1116	0	+ 401	+ 182	
				Impact No. 18; t = 14.6 sec.		
S	−1435	−1845	+1338			
S_x	0	0	+1090	+1090	+ 527	
S_y	−1291	−1661	+ 773	−2179	−2179	2243
S_z	− 625	+ 804	0	+ 179	+ 81	
				Impact No. 19; t = 15 sec.		
S	−2150	−1230	+1876			
S_x	0	0	+1529	+1529	+ 740	
S_y	−1935	1108	+1084	−1959	−1959	2102
S_z	− 937	+ 536	0	− 401	− 182	
				Impact No. 20; t = 16.15 sec.		
S	−1947	−1538	+1680			
S_x	0	0	+1310	+1310	+ 634	
S_y	−1752	−1384	+ 928	−2208	−2208	2299
S_z	− 848	+ 670	0	− 178	− 81	
				Impact No. 21; t = 16.9 sec.		
S	−2560	−1743	+1338			
S_x	0	0	+1090	+1090	+ 527	
S_y	−2304	−1569	+ 773	−3100	−3100	3149
S_z	−1116	+ 760	0	− 356	− 162	
				Impact No. 22; t = 17.5 sec.		
S	−1230	−2151	+2680			
S_x	0	0	+2184	+2184	+1056	
S_y	−1107	−1936	+1549	−1494	−1494	1839
S_z	− 536	+ 937	0	+ 401	+ 182	
				Impact No. 23; t = 17.9 sec.		
S	−1025	−1025	+1472			
S_x	0	0	+1200	+1200	+580	
S_y	− 922	− 922	+ 850	− 994	−994	1155
S_z	− 447	+ 447	0	0	0	

Landing No. 2, Airplane No. 1

	0–3'	0–3	1–4	Σ	KΣ	P
				Impact No. 1; t = 0 sec.		
S	−1435	−1735	−804	Σ	KΣ	P
S_x	0	0	−656	− 656	− 318.	
S_y	−1292	−1562	−466	−3320	−3320	3336
S_z	− 625	+ 757	0	+ 142	65	
				Impact No. 2; t = 1.72 sec.		
S	−1435	−1435	−668			
S_x	0	0	−545	− 545	− 264	
S_y	−1292	−1292	−386	−2970	−2970	2982
S_z	− 625	+ 625	0	0	0	
				Impact No. 3; t = 2.58 sec.		
S	−1538	−1590	−536			
S_x	0	0	−437	− 437	− 212	
S_y	−1384	−1431	−309	−3124	−3124	3131
S_z	− 670	+ 693	0	+ 23	+ 11	
				Impact No. 4; t = 3.7 sec.		
S	−2563	−3075	−1608			
S_x	0	0	−1310	−1310	− 634	
S_y	−2307	−2768	− 929	−6004	−6004	6038
S_z	−1117	+1341	0	+ 224	+ 102	
				Impact No. 5; t = 5.3 sec.		
S	−2040	+2050	−668			
S_x	0	0	−545	− 545	−264	
S_y	−1842	+1845	−387	− 384	−384	940
S_z	− 893	− 894	~0	−1787	−815	
				Impact No. 6; t = 6.15 sec.		
S	−2050	+1435	+804			
S_x	0	0	+655	+ 655	+317	
S_y	− 1845	+1290	+465	− 90	− 90	766
S_z	− 894	− 626	0	−1520	−691	
				Impact No. 7; t = 6.85 sec.		
S	−2255	−1538	+936			
S_x	0	0	+763	+ 763	+ 370	
S_y	−2030	−1384	+541	−2873	−2873	2900
S_z	− 983	+ 671	0	− 312	− 142	
				Impact No. 8; t = 8.15 sec.		
S	−2665	−1538	+1474			
S_x	0	0	+1201	+1201	+ 581	
S_y	−2399	−1384	853	−2930	−2930	2995
S_z	−1162	+ 671	0	− 491	− 224	
	0–3'	0–3	1–4	Impact No. 9; t = 8.7 sec.		
S	−2563	−2050	+1340	Σ	KΣ	P
S_x	0	0	+1091	+1091	+ 528	
S_y	−2307	−1845	774	−3378	−3378	3420
S_z	−1117	+ 894	0	− 223	− 101	
				Impact No. 10; t = 10.4 sec.		
S	−718	−513	−536			
S_x	0	0	−437	− 437	− 211	
S_y	−647	−462	−310	−1419	−1419	1435
S_z	−313	+224	0	− 89	− 40	

Landing No. 3, Airplane No. 1

	0–3′	0–3	1–4	Σ	KΣ	P
				Impact No. 1; t=0 sec.		
S	−1230	−2255	−1205			
S_x	0	0	− 982	− 982	− 475	
S_y	−1107	−2030	− 696	−3833	−3833	3867
S_z	− 536	+ 983	0	+ 447	+ 203	
				Impact No. 2; t=2 sec.		
S	−1230	−3075	−1072			
S_x	0	0	− 874	− 874	− 423	
S_y	−1107	2767	− 620	−4494	−4494	4529
S_z	− 536	+1341	0	+ 805	− 366	
				Impact No. 3; t=3.5sec.		
S	−1025	−2560	−804			
S_x	0	0	−655	− 655	− 317	
S_y	− 920	−2305	−465	−3690	−3690	3720
S_z	− 447	+1118	0	+ 671	− 355	
				Impact No. 4; t=4.72sec.		
S	−1230	−2560	−536			
S_x	0	0	−437	− 437	− 211	
S_y	−1107	−2305	−310	−3722	−3722	3746
S_z	− 536	+1118	0	+ 682	+ 310	
				Impact No. 5; t=5.73sec.		
S	−3075	−3075	−268			
S_x	0	0	−218	− 218	− 105	
S_y	−2767	−2767	−155	−5689	−5689	5690
S_z	−1341	+1341	0	0	0	
				Impact No. 6; t=6.43 sec.		
S	−1127	−2050	−536			
S_x	0	0	−437	− 436	− 211	
S_y	−1014	−1847	−311	−3172	−3172	3184
S_z	− 492	+ 894	0	+ 402	+ 183	
				Impact No. 7; t=7.3sec.		
S	−1127	−2050	+1205			
S_x	0	0	+ 982	+ 982	+ 475	
S_y	−1014	−1847	+ 692	−2169	−2169	2228
S_z	− 492	+ 894	0	+ 402	+ 183	
				Impact No. 8; t=8.58sec.		
S	−1230	+1640	−1338			
S_x	0	0	−1090	−1090	−527	
S_y	−1105	+1475	774	− 404	−404	873
S_z	− 536	− 714	0	−1250	−567	
				Impact No.9; t=9.3 sec.		
S	−1846	+512	−1338			
S_x	0	0	−1090	−1090	− 527	
S_y	−1662	461	− 774	−1974	−1974	2061
S_z	− 805	224	0	− 581	− 264	
				Impact No.10; t=10 sec.		
S	−3075	−2050	−669			
S_x	0	0	−545	− 545	− 264	
S_y	−2775	−1850	−388	−5013	−5013	5024
S_z	−1340	+ 893	0	− 447	− 204	
				Impact No.11; t=10.5 sec.		
S	−2150	−3385	−1338			
S_x	0	0	−1090	−1090	− 527	
S_y	−1935	−3045	− 773	−5753	−5753	5782
S_z	− 937	+1478	0	+ 541	+ 241	
				Impact No.12; t=12 sec.		
S	−1640	−3075	−1606			
S_x	0	0	−1310	−1310	−634	
S_y	−1480	−2775	− 928	−5183	−5183	5229
S_z	− 715	+1340	0	+ 625	+ 285	
				Impact No. 13; t=13.4sec.		
S	−615	−1538	−536			
S_x	0	0	−437	− 437	− 212	
S_y	−555	−1388	−310	−2253	−2253	2269
S_z	−242	+ 605	0	+ 363	+ 165	

Take-off No. 1, airplane No. 1

	0–3′	0–3	1–4	Σ	KΣ	P
				Impact No. 1; t=0 sec.		
S	−1538	−1025	−670			
S_x	0	0	−546	− 546	− 265	
S_y	−1384	− 923	−388	−2695	−2695	2710
S_z	− 670	+ 447	0	− 223	− 101	
				Impact No. 2; t=0.6 sec.		
S	−1950	−2255	−936			
S_x	0	0	−752	− 752	− 362	
S_y	−1754	−2030	−541	−4325	−4325	
S_z	− 850	+ 981	0	+ 131	+ 59	4315
				Impact No.3; t=1.4 sec.		
S	−1640	−2050	−806			
S_x	0	0	−655	− 655	− 317	
S_y	−1477	−1847	−465	−3789	−3789	3803
S_z	− 714	+ 893	0	+ 179	+ 84	
				Impact No.4; t=2.4sec.		
S	−2050	−3075	−936			
S_x	0	0	−752	− 752	− 364	
S_y	−1847	−2770	−541	−5158	−5158	5175
S_z	− 893	+1343	0	+ 450	+ 205	
				Impact No.5; t=4.47sec.		
S	−1845	−2255	−1205			
S_x	0	0	− 981	− 981	− 475	
S_y	−1660	−2030	− 697	−4387	−4387	4413
S_z	− 804	+ 981	0	+ 177	+ 87	
				Impact No.6; t=5.43 sec.		
S	−1742	−1538	−536			
S_x	0	0	−437	− 437	− 211	
S_y	−1568	−1384	−310	−3262	−3262	3269
S_z	− 758	+ 670	0	− 88	− 40	
				Impact No.7; t=6.58 sec.		
S	−1128	−1538	−670			
S_x	0	0	−546	− 546	− 264	
S_y	−1015	−1384	−387	−2786	−2786	2799
S_z	− 492	+ 670	0	+ 178	+ 78	
				Impact No.8; t=8.34 sec.		
S	−1538	−2050	−804			
S_x	0	0	−655	− 655	− 317	
S_y	−1384	−1845	−455	−3686	−3686	3701
S_z	− 670	+ 893	0	+ 223	+ 101	

Take-off No.2, airplane No.1

	0–3′	0–3	1–4	Σ	KΣ	P
				Impact No.1; t=0 sec.		
S	−2252	−1640	+936			
S_x	0	0	764	+ 764	+ 370	
S_y	−2027	−1476	+445	−3058	−3058	3083
S_z	− 982	+ 715	0	− 267	− 122	
				Impact No.2; t=0.71 sec.		
S	−1230	−2050	−404			
S_x	0	0	−329	− 329	− 159	
S_y	−1107	−1845	−234	−3186	−3186	3194
S_z	− 536	+ 894	0	+ 358	+ 163	
				Impact No.3; t=1.14sec.		
S	−1538	−2050	−404			
S_x	0	0	−329	− 329	− 159	
S_y	−1384	−1845	−234	−3463	−3463	3467
S_z	− 671	+ 894	0	+ 223	+ 101	
				Impact No.4; t=1.71sec.		
S	−1435	−2050	−268			
S_x	0	0	−219	− 219	− 106	
S_y	−1292	−1845	−155	−3292	−3292	3296
S_z	− 626	+ 894	0	+ 268	+ 122	
				Impact No.5; t=2.29sec.		
S	−2560	−3582	+1205			
S_x	0	0	+ 982	+ 982	+ 476	
S_y	−2304	−3224	+ 697	−4831	−4831	4859
S_z	−1116	+1562	0	+ 446	+ 203	
				Impact No.6; t=2.86sec.		
S	−2050	−3075	+1606			
S_x	0	0	+1310	+1310	+ 631	
S_y	−1845	−2768	+ 929	−3684	−3684	3735
S_z	− 894	+1341	0	+ 442	+ 204	
				Impact No.7; t=3.57sec.		
S	−1230	−2560	−404			
S_x	0	0	−329	− 329	− 159	
S_y	−1107	−2304	−234	−3645	−3645	3658
S_z	− 536	+1116	0	+ 580	+ 264	
				Impact No.8; t=4.28sec.		
S	−1025	−2460	−404			
S_x	0	0	−329	− 329	− 159	
S_y	− 922	−2214	−234	−3370	−3370	3386
S_z	− 447	+1072	0	+ 625	+ 285	
	0–3′	**0–3**	**1–4**	**Impact No.9; t=4.85sec.**		
				Σ	KΣ	P
S	−1025	−2560	−404			
S_x	0	0	−329	− 329	− 159	
S_y	− 922	−2304	−234	−3460	−3460	3477
S_z	− 447	+1116	0	+669	+ 304	
				Impact No.10; t=5.42sec.		
S	−512	−1025	−404			
S_x	0	0	−329	− 329	− 159	
S_y	−461	− 922	−234	−1617	−1617	1628
S_z	−224	+ 447	0	+ 223	+ 101	
				Impact No.11; t=5.71sec.		
S	−1025	−2560	−404			
S_x	0	0	−329	− 329	− 159	
S_y	− 922	−2304	−234	−3460	−3460	3477
S_z	− 447	+1116	0	+ 669	+ 304	
				Impact No.12; t=7 sec.		
S	−1358	−2560	−536			
S_x	0	0	−437	− 437	− 211	
S_y	−1222	−3384	−311	−3837	−3837	3850
S_z	− 592	+1116	0	+ 524	+ 239	
				Impact No.13; t=8.55sec.		
S	−1025	−2560	0			
S_x	0	0	0	0	0	
S_y	− 922	−2304	0	−3226	−3226	3237
S_z	− 447	+1116	0	+ 669	+ 304	
				Impact No.14; t=10.3sec.		
S	−1025	−1538	−1072			
S_x	0	0	− 874	− 874	− 425	
S_y	− 922	−1385	− 620	−2927	−2927	2958
S_z	− 447	+ 678	0	+ 231	+ 105	

Take-off No.3, Airplane No.1

	0—3'	0—3	1—4	Impact No.1;t=0sec.		
S	−1 230	−1 538	−536	Σ	KΣ	P
S_x	0	0	−437	− 437	− 211	
S_y	−1 107	−1 384	−310	−2 801	−2 801	2 009
S_z	− 536	+ 670	0	+ 134	+ 61	
S	−1 230	−1 845	+536	Impact No.2;t=1.86sec.		
S_x	0	0	+437	+ 437	+ 211	
S_y	−1 107	−1 476	−310	−2 273	−2 273	2 286
S_z	− 536	+ 805	0	+ 269	+ 123	
S	−1 230	−1 640	+268	Impact No.3;t=3.29sec.		
S_x	0	0	+218	+ 218	+ 106	
S_y	−1 107	−1 475	+155	−2 427	−2 427	2 431
S_z	− 536	+ 716	0	+ 180	+ 92	
S	−2 252	−3 075	+804	Impact No.4;t=4.43sec.		
S_x	0	0	+655	+ 655	+ 317	
S_y	−2 029	−2 767	+465	−4 331	−4 331	4 347
S_z	− 982	+1 340	0	+ 358	+ 163	
S	−1 743	−1 946	+404	Impact No.5;t=6.72sec.		
S_x	0	0	+329	+ 329	+ 159	
S_y	−1 570	−1 753	+234	−3 089	−3 089	3 093
S_z	− 759	− 848	0	+ 89	+ 41	
S	−1 334	−2 560	+268	Impact No.6;t=8.15sec.		
S_x	0	0	+218	+ 218	+ 105	
S_y	−1 200	−2 300	+149	−3 351	−3 351	3 361
S_z	− 581	+1 117	0	+ 536	+ 244	
S	0	2 050	0	Impact No.7;t=10 sec.		
S_x	0	0	0	0	—	
S_y	0	−1 846	0	−1 846	−1 846	1 890
S_z	0	+ 893	0	+ 893	+ 407	

Take-off No.4; airplane No.1

	0—3'	0—3	1—4	Impact No.1;t=0sec.		
S	−1 025	−1 230	0	Σ	KΣ	P
S_x	0	0	0	0	0	
S_y	− 923	−1 107	0	−2 030	−2 030	2 031
S_z	− 447	+ 536	0	+ 89	+ 40	
S	−1 538	−1 435	−268	Impact No.2;t=1.57sec.		
S_x	0	0	−218	− 218	− 105	
S_y	−1 383	−1 290	−155	−2 828	−2 828	2 830
S_z	− 670	+ 625	0	− 45	− 20	
S	−1 435	−1 946	−404	Impact No.3;t=2.15sec.		
S_x	0	0	−329	− 329	− 159	
S_y	−1 290	−1 750	−234	−3 274	−3 274	3 279
S_z	− 625	+ 848	0	+ 223	+ 101	
S	−1 640	−1 130	−134	Impact No.4;t=4 sec.		
S_x	0	0	−109	− 109	− 53	
S_y	−1 480	−1 016	−775	−3 271	−3 271	3 273
S_z	− 715	+ 493	0	− 222	− 101	
S	−2 050	−1 946	−268	Impact No.5;t=5.15sec.		
S_x	0	0	−218	− 218	− 105	
S_y	−1 844	−1 750	−149	−3 743	−3 743	3 744
S_z	− 895	+ 848	0	− 47	− 21	
S	−1 025	−1 743	0	Impact No.6;t=7.15sec.		
S_x	0	0	0	0	0	
S_y	− 922	−1 569	0	−2 491	−2 491	2 495
S_z	− 447	+ 762	0	+ 315	+ 143	
S	−1 230	−1 538	−670	Impact No.7;t=8.3 sec.		
S_x	0	0	−546	− 546	− 264	
S_y	−1 116	−1 384	−388	−2 878	−2 878	2 890
S_z	− 536	+ 670	0	+ 134	+ 61	
S	−718	−1 743	−134	Impact No.8;t=9.3 sec.		
S_x	0	0	−109	− 109	− 53	
S_y	−646	−1 568	− 77	−2 291	−2 291	2 305
S_z	−313	+ 760	0	+ 447	+ 203	
S	−922	−1 435	−404	Impact No.9;t=10.85 sec.		
S_x	0	0	−329	− 329	− 159	
S_y	−830	−1 290	−234	−2 354	−2 354	2 361
S_z	−402	+ 625	0	+ 223	+ 101	

Appendix 2

Table of forces in struts of landing gears No.2 and their components in the X and Y direction.

Landing No. 1

	Пер. нога	Задн. нога	Кабаны			
	1—2	1—3	4—2	4—2'	Σ	KΣ
S	− 735	+788	−1 182	+1 445	Impact No.1;t=1.8	
S_x	130	+616	—	—	746	− 746
S_y	− 630	—	—	—	− 630	531
S	−1 960	+656	−1 840	−1 315	Impact No.2;t=2.8	
S_x	345	+512	—	—	857	−857
S_y	−1 681	—	—	—	−1 681	1 420
S	−1 225	−656	−1 970	− 920	Impact No.3;t=3.2	
S_x	216	−512	—	—	− 296	296
S_y	−1 050	—	—	—	−1 050	887
S	−1 225	+394	+1 050	−1 050	Impact No.4;t=3.8	
S_x	216	308	—	—	524	−524
S_y	−1 050	—	—	—	−1 050	887
S	−2 203	+526	−1 315	− 656	Impact No.5;t=4.6	
S_x	392	+411	—	—	9	−9
S_y	−1 915	—	—	—	−1 915	1 616
S	−1 225	+394	−1 445	−1 182	Impact No.6;t=5.1	
S_x	216	308	—	—	524	−524
S_y	−1 050	—	—	—	−1 050	827
S	− 980	+394	− 525	+ 526	Impact No.7;t=6.1	
S_x	173	308	—	—	481	−481
S_y	− 840		—	—	− 840	708
S	−1 750	−920	+ 920	+1 445	Impact No.8;t=7.1	
S_x	308	−718	—	—	− 410	410
S_y	−1 502	—	—	—	−1 502	1 268
S	−2 940	−394	−1 580	−1 315	Impact No.9;t=7.7	
S_x	517	−308	—	—	209	−209
S_y	−2 520	—	—	—	−2 520	2 121
S	−1 715	−788	−1 315	−2 100	Impact No.10;t=8.1	
S_x	302	−616	—	—	− 314	314
S_y	−1 470	—	—	—	−1 470	1 241
S	−2 450	$\boxed{-1\,182}$	+1 580	− 920	Impact No.11;t=8.6	
S_x	431	− 923	—	—	− 492	492
S_y	−2 100	—	—	—	−2 100	1 772
S	−2 940	+ 526	+1 315	$\boxed{-2\,235}$	Impact No.12;t=9.1	
S_x	517	411	—	—	928	− 928
S_y	−2 520	—	—	—	−2 520	2 121
S	−2 940	− 788	−1 315	−1 050	Impact No.13;t=9.7	
S_x	517	− 616	—	—	− 99	99
S_y	−2 520	—	—	—	−2 520	2 121
S	−1 715	− 788	+1 445	−1 182	Impact No.14;t=10.1	
S_x	302	− 616	—	—	− 314	314
S_y	−1 470	—	—	—	−1 470	1 241
S	− 735	− 656	+ 920	− 788	Impact No.15;t=10.8	
S_x	129	− 512	—	—	− 383	383
S_y	− 630	—	—	—	− 630	531

Landing No. 2

S	−2 450	+ 132	−1 315	−1 315	Impact No.1; t= 0	
S_x	+ 431	+ 103	—	—	+ 534	− 534
S_y	−2 100	—	—	—	−2 100	+1 770
S	− 735	+ 263	−1 315	−1 315	Impact No.2; t=1	
S_x	+ 129	+ 205	—	—	+ 334	− 334
S_y	− 630	—	—	—	− 630	+ 531
S	−1 960	+ 525	−1 580	−2 150	Impact No.3;t=1.8	
S_x	+ 340	+ 410	—	—	+ 750	− 750
S_y	−1 680	—	—	—	−1 680	+1 415
S	−2 205	+ 788	+1 580	− 788	Impact No.4;t=2.4	
S_x	+ 388	+ 615	—	—	+1 003	−1 003
S_y	−1 890	—	—	—	−1 890	+1 593
S	−1 225	+ 263	+1 580	−1 050	Impact No.5;t=2.9	
S_x	+ 216	+ 205	—	—	+ 421	− 421
S_y	−1 050	—	—	—	−1 050	+ 885

Landing No. 2

	1—2	1—3	4—2	4—2'	Σ	KΣ
S	−1225	−788	−2235	−1050	Impact No.6;t=3.5	
S_x	+ 216	−615	—	—	− 399	+ 399
S_y	−1050	—	—	—	−1050	+ 885
S	−2450	+263	+1315	− 526	Impact No.7;t=4	
S_x	+ 431	+205	—	—	+ 636	− 636
S_y	−2100	—	—	—	−2100	+1770
S	−1715	−263	−1050	+1315	Impact No.8;t=4.8	
S_x	+ 302	−205	—	—	+ 97	− 97
S_y	−1470	—	—	—	−1470	+1240
S	−1715	+656	−1050	− 788	Impact No.9;t=5.1	
S_x	+ 302	+512	—	—	+ 814	− 814
S_y	−1470	—	—	—	−1470	+1240
S	−1470	+526	− 788	− 526	Impact No.10;t=5.9	
S_x	+ 258	+411	—	—	+ 669	− 669
S_y	−1260	—	—	—	−1200	+1062
S	−2450	+263	− 920	+ 920	Impact No.11;t=6.1	
S_x	+ 431	+205	—	—	+ 636	− 636
S_y	−2100	—	—	—	−2100	+1770
S	−1715	−394	+ 920	+1315	Impact No.12;t=6.6	
S_x	+ 302	−307	—	—	− 5	+ 5
S_y	−1470	—	—	—	−1470	+1240
S	−1715	−263	− 788	+1315	Impact No.13;t=7.1	
S_x	+ 302	−205	—	—	+ 97	− 97
S_y	−1470	—	—	—	−1470	+1240
S	−2700	−263	+ 788	+1315	Impact No.14;t=7.5	
S_x	+ 475	−205	—	—	+ 270	− 270
S_y	−2316	—	—	—	−2316	+1950
S	−2940	−394	+1050	+1050	Impact No.15;t=8.1	
S_x	+ 517	−307	—	—	+ 210	− 210
S_y	−2520	—	—	—	−2520	+2123
S	−2700	−263	+ 788	+1445	Impact No.16;t=8.6	
S_x	+ 475	−205	—	—	+ 270	− 270
S_y	−2316	—	—	—	−2316	+1950
S	−2940	−526	+ 788	+1445	Impact No.17;t=8.8	
S_x	+ 517	−411	—	—	+ 106	− 106
S_y	−2520	—	—	—	−2520	+2123
S	−3430	+394	+1050	+1445	Impact No.18;t=9.6	
S_x	+ 604	+307	—	—	+ 911	− 911
S_y	−2940	—	—	—	−2940	+2480
S	−2450	−656	+1445	+1315	Impact No,19;t=10.2	
S_x	+ 431	−512	—	—	− 81	+ 81
S_y	−2100	—	—	—	−2100	+1770
S	−3680	−334	+ 920	+1445	Impact No.20;t=10.7	
S_x	+ 647	−262	—	—	+ 385	− 385
S_y	−3154	—	—	—	−3154	+2659
S	−2450	+132	+ 920	+1315	Impact No.21;t=11.2	
S_x	+ 431	+103	—	—	+ 534	− 534
S_y	−2100	—	—	—	−2100	+1770

Take-off No. 1

	1—2	1—3	4—2	4—2'	Σ	KΣ
S	−1470	−263	656	656	Impact No.1; t=0	
S_x	258	− 205	—	—	53	− 53
S_y	−1260	—	—	—	−1260	+1060
S	− 980	−656	1050	394	Impact No.2;t=0.7	
S_x	173	−512	—	—	− 333	+ 339
S_y	− 840	—	—	—	− 840	+ 708
S	−1470	−789	656	656	Impact No.3;t=1.0	
S_x	288	−616	—	—	− 358	+ 358
S_y	−1260	—	—	—	−1260	+1060
S	−1225	−525	1313	920	Impact No.4;t=1.4	
S_x	216	−410	—	—	− 194	+ 194
S_y	−1050	—	—	—	−1050	+ 884
S	−2450	−394	1970	1182	Impact No.5;t=2.2	
S_x	431	−308	—	—	123	− 123
S_y	−2100	—	—	—	−2100	+1773
S	−2450	− 394	788	1050	Impact No.6;t=2.8	
S_x	431	− 308	—	—	− 123	+ 123
S_y	−2100	—	—	—	−2100	+1773
S	−2205	− 676	1313	1182	Impact No.7;t=3.4	
S_x	388	−512	—	—	− 123	+ 123
S_y	−1892	—	—	—	−1892	+1595
S	−1715	−656	2100	1313	Impact No.8;t 3.8	
S_x	302	−512	—	—	− 210	+ 210
S_y	−1470	—	—	—	−1470	+1240
S	− 980	−656	1313	1313	Impact No.9;t=4.2	
S_x	173	−512	—	—	− 339	+ 339
S_y	− 840	—	—	—	− 810	+ 708
S	−2450	−789	1840	−1050	Impact No.10;t=5	
S_x	431	−616	—	—	− 185	+ 185
S_y	−2100	—	—	—	2100	+1772
S	− 735	−920	1970	2365	Impact No.11;t=5.7	
S_x	130	−718	—	—	− 588	− 588
S_y	− 630	—	—	—	− 630	− 531

Take-off No.2

	1—2	1—3	4—2	4—2'	Σ	KΣ
S	−1470	−394	2105	2105	Impact No.1;t=0.34	
S_x	258	−308	—	—	− 50	+ 50
S_y	−1260	—	—	—	−1260	+1064
S	−1715	−920	1315	− 789	Impact No.2;t=1.1	
S_x	302	−718	—	—	− 316	+ 316
S_y	−1470	—	—	—	−1470	+1242
S	−1470	−789	789	− 789	Impact No.3;t=1.6	
S_x	258	−616	—	—	− 358	+ 358
S_y	−1260	—	—	—	−1260	+1064
S	−1470	+789	− 789	−1448	Impact No.4;t=2.1	
S_x	− 258	−616	—	—	− 874	+ 874
S_y	−1260	—	—	—	−1260	+1064
S	−1470	+789	−1315	−2105	Impact No.5;t=2.7	
S_x	258	−616	—	—	− 358	+ 358
S_y	−1260	—	—	—	−1260	+1064
S	− 490	−394	1315	−1050	Impact No.6;t=3.8	
S_x	86	−308	—	—	− 222	+ 222
S_y	− 425	—	—	—	− 425	+ 359

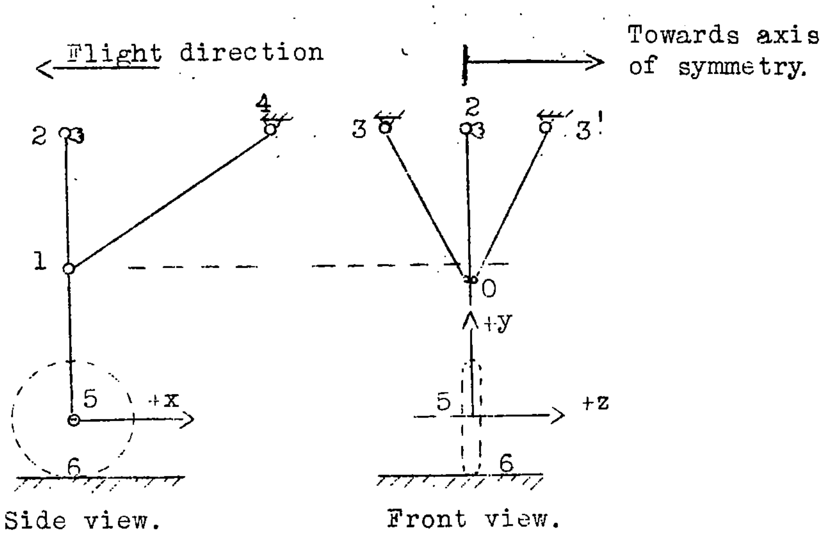

Member	length 1 cm	cos (1x)	cos (1y)	cos (1_z)
0-3	980	.0	.90	-.436
0-3	980	.0	.90	.436
1-4	1352	.815	.578	.0

Figure 1.- Arrangement of landing gear of airplane no. 1.

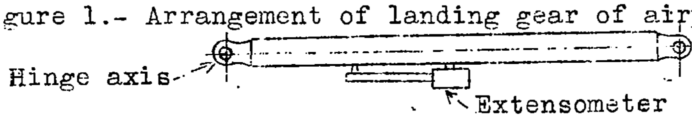

Figure 2.- Showing how extensometer is placed on strut.

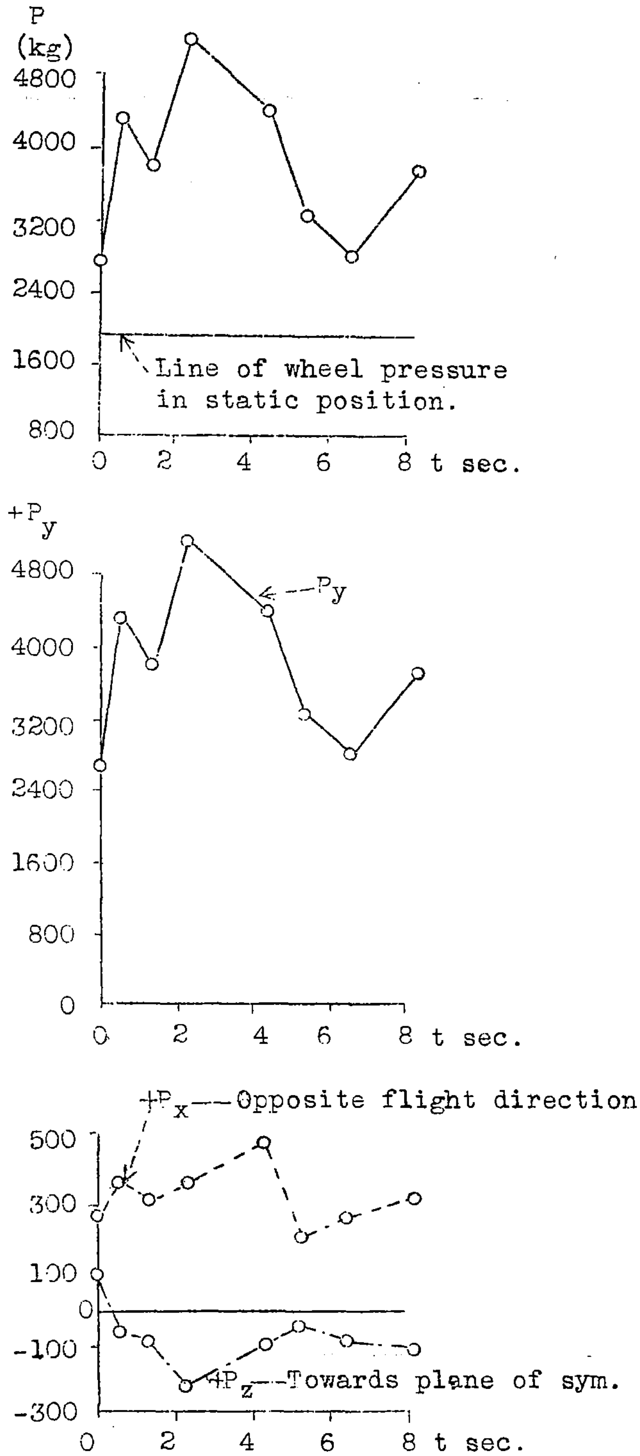

t sec	P kg.
0	2,710
0.6	4,345
1.4	3,803
2.4	5,175
4.47	4,413
5.43	3,269
6.58	2,799
8.34	3,701

t sec	P_x	P_y	P_z
0	265	2,695	101
0.6	362	4,325	-59
1.4	317	3,789	-84
2.4	364	5,158	-205
4.47	475	4,387	-87
5.43	211	3,262	40
6.58	264	2,786	-78
8.34	317	3,686	-101

Figure 3.- Time history of external force P on wheel of airplane no. 1 (take-off no. 1).

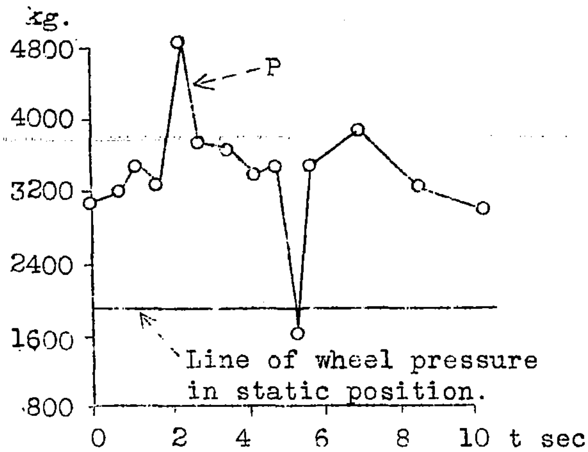

t sec.	P kg.
0	3,083
0.71	3,194
1.14	3,467
1.71	3,296
2.29	4,859
2.86	3,735
3.57	3,658
4.28	3,386
4.85	3,477
5.42	1.628
5.71	3,477
7	3,850
8.55	3,237
10.3	2,958

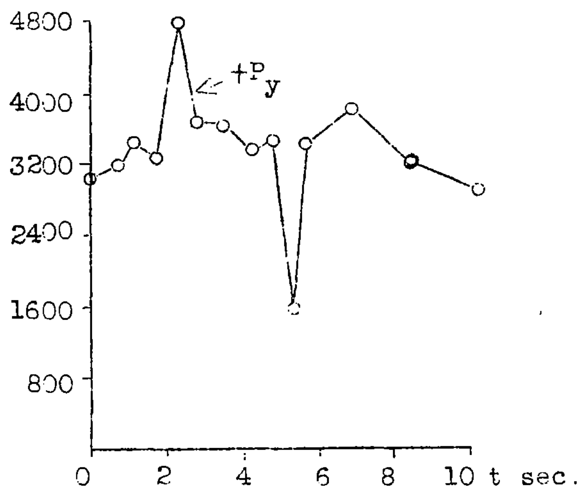

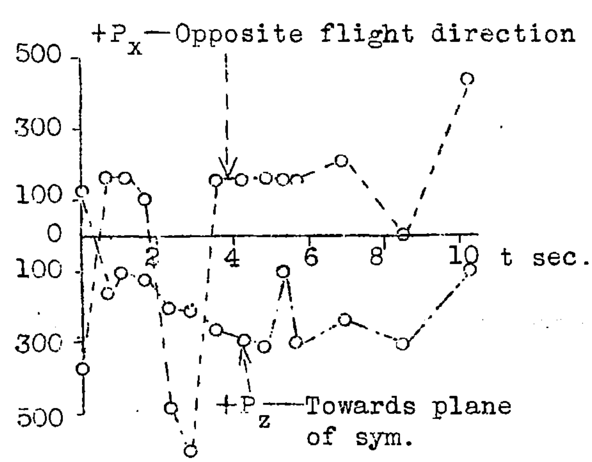

t sec.	P_x	P_y	P_z
0	-370	3,058	122
0.71	+159	3,186	-163
1.14	+159	3,463	-101
1.71	+106	3,292	-122
2.29	-476	4,831	-203
2.86	-631	3,684	-204
3.57	+159	3,645	-264
4.28	+159	3,370	-285
4.85	+159	3,460	-304
5.42	+159	1,617	-101
5.71	+159	3,460	-304
7	+ 211	3,837	-239
8.55	0	3,226	-304
10.3	+425	2,927	-105

Figure 4.- Time history of external force P on wheel of airplane no. 1 (take-off no. 2).

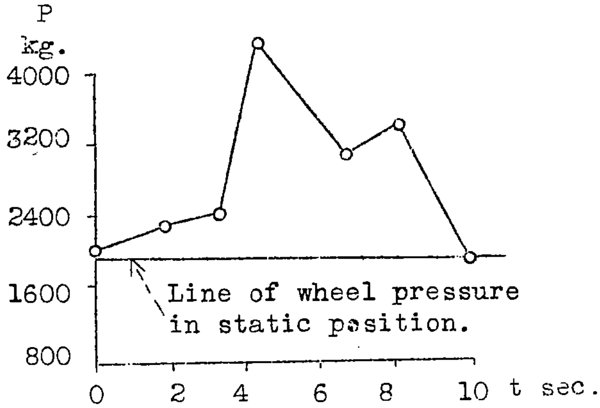

t sec.	P kg.
0	2,009
1.86	2,286
3.29	2,431
4.43	4,347
6.72	3,093
8.15	3,361
10	1,890

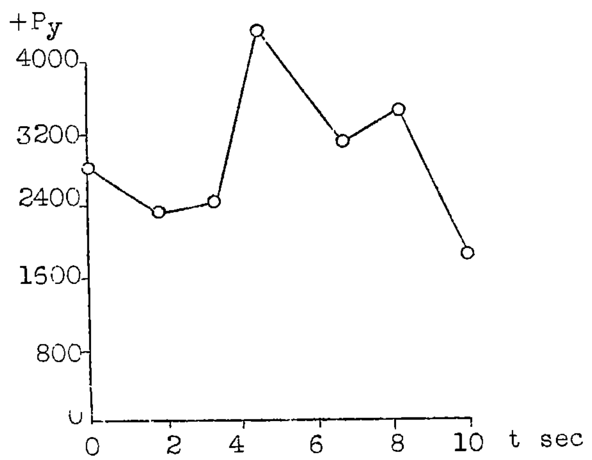

t sec	P_x	P_y	P_z
0	211	2,801	-61
1.86	-211	2,273	-123
3.29	-106	2,427	-92
4.43	-317	4,331	-163
6.72	-159	3,089	-41
8.15	-105	3,351	-244
10	0	1,846	-407

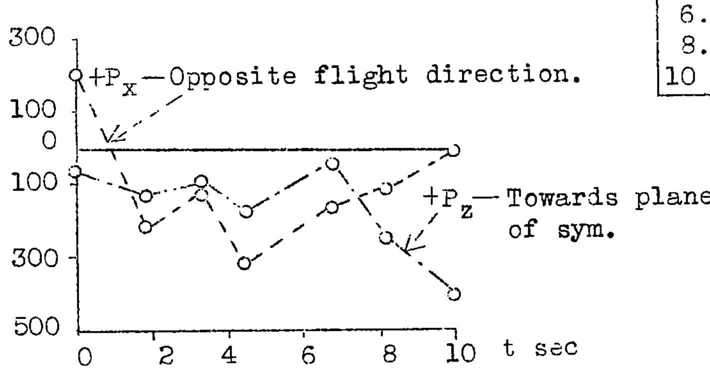

Figure 5.- Time history of external force P on landing-gear wheel of airplane no. 1 (take-off 3).

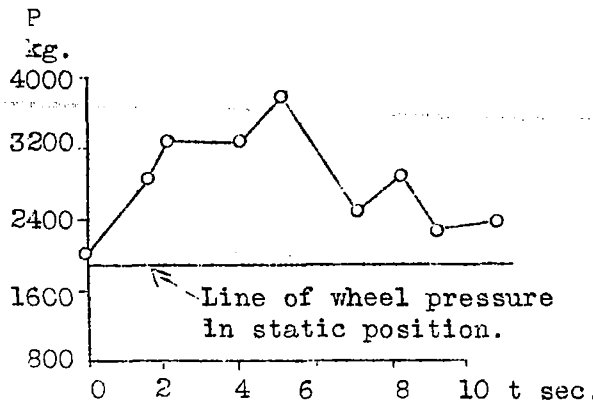

t sec.	P kg.
0	2,031
1.57	2,830
2.15	3,279
4	3,273
5.15	3,744
7.15	2,495
8.3	2,890
9.3	2,305
10.85	2,361

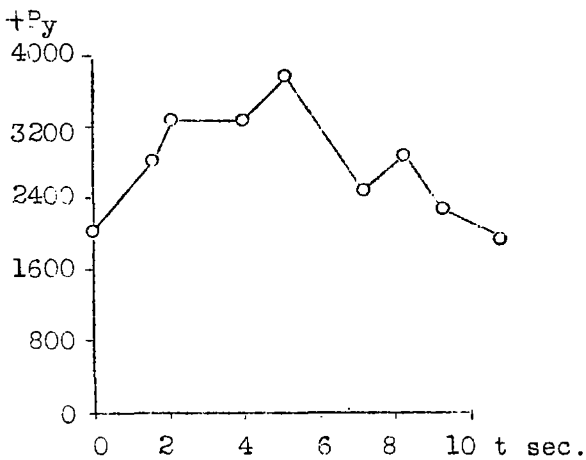

t sec.	P_x	P_y	P_z
0	0	2,030	-41
1.57	105	2,828	-20
2.15	159	3,274	-101
4	53	3,271	101
5.15	105	3,743	21
7.15	0	2,491	-143
8.3	264	2,878	-61
9.3	53	2,291	-203
10.85	159	2,354	-101

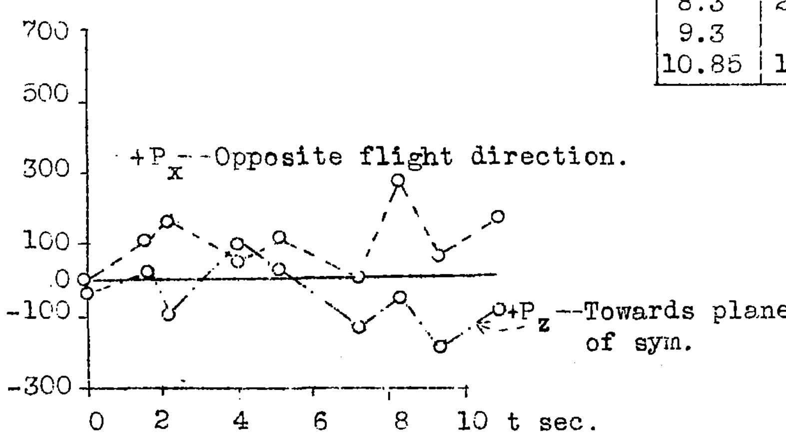

Figure 6.- Time history of vertical and horizontal components of pressure on landing-gear wheel of airplane no. 1 (take-off).

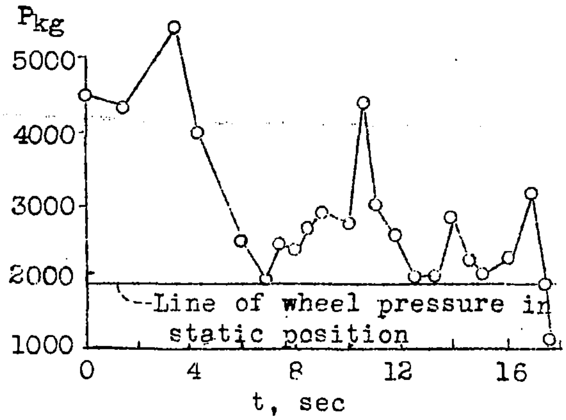

t_{sec}	P_{kg}	t_{sec}	P_{kg}
0	4509	11.15	3038
1.5	4372	11.75	2594
3.5	5468	12.45	2166
4.7	4013	13.25	2099
6.0	2543	13.90	2804
6.7	2017	14.6	2243
7.35	2488	15.0	2102
8.0	2354	16.15	2299
8.5	2697	16.9	3149
9.0	2954	17.5	1839
10.0	2764	17.9	1155
10.5	4419		

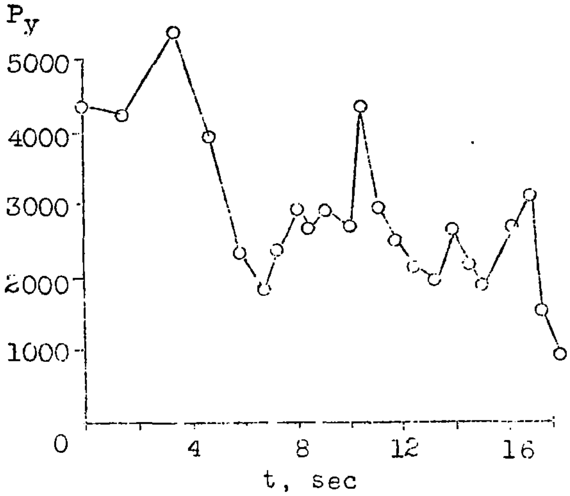

t_{sec}	P_x	P_y	P_z
0	-586	4436	-428
1.5	-796	4274	-467
3.5	-634	5431	24
4.7	-369	3978	224
6.0	-740	2421	243
6.7	-740	1865	203
7.35	-475	2441	81
8.0	-263	2842	- 61
8.5	-263	2680	-141
9.0	-263	2842	- 61
10.0	-475	2719	-142
10.5	-527	4386	-122
11.15	-686	2959	- 60
11.75	-686	2501	- 41
12.45	-369	2134	- 20
13.25	-423	2056	- 20
13.9	-740	2699	-182
14.6	-527	2179	- 81
15.0	-740	1959	182
16.15	-634	2208	81
16.9	-527	3100	162
17.5	-1056	1494	-182
17.9	-580	994	0

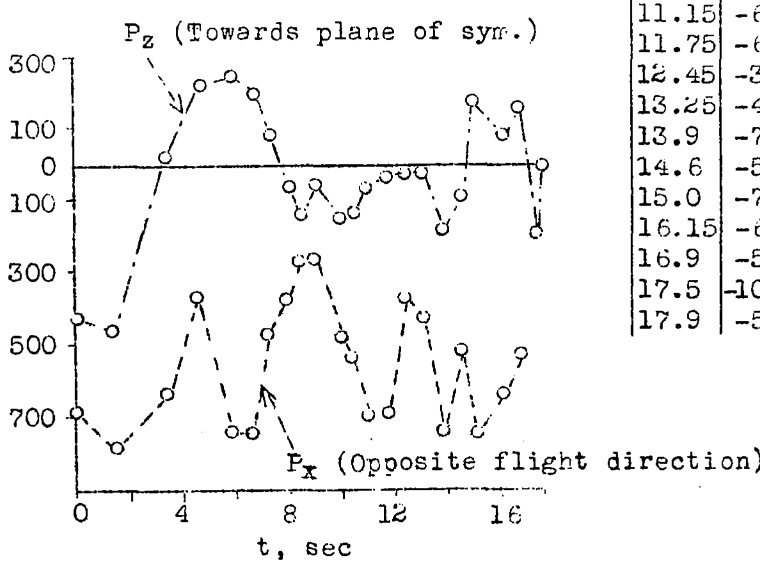

Figure 7.- Time history of vertical and horizontal components of pressure on landing-gear wheel of airplane No. 1. (landing 1).

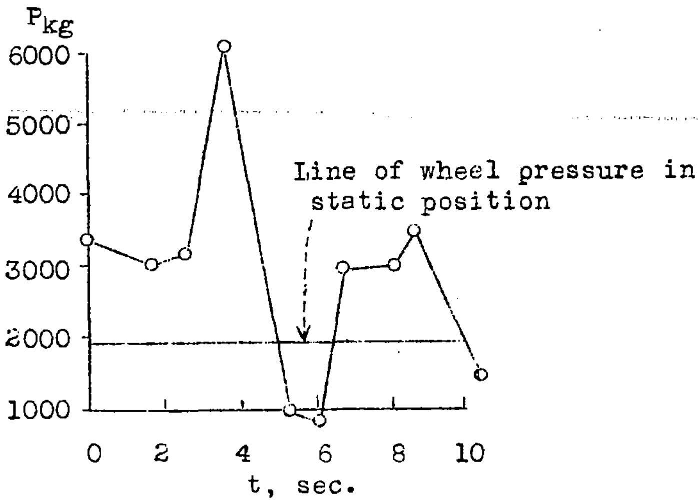

$t_{sec.}$	P_{kg}
0	3336
1.72	2982
2.58	3131
3.7	6038
5.3	940
6.15	766
6.85	2900
8.15	2995
8.7	3420
10.4	1435

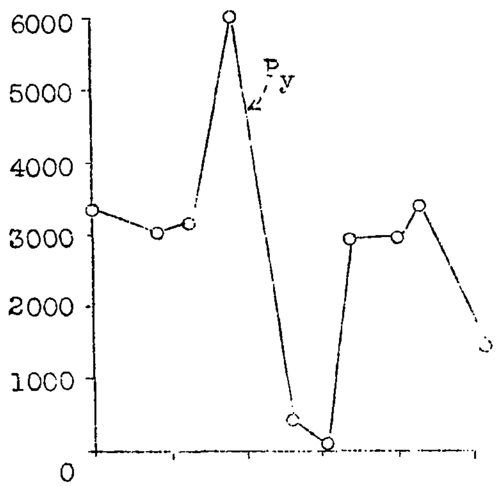

$t_{sec.}$	P_x	P_y	P_z
0	318	3320	- 65
1.72	254	2970	0
2.58	212	3124	- 11
3.7	634	6004	-102
5.3	264	387	815
6.15	-317	90	691
6.85	-370	2873	142
8.15	-581	2930	224
8.7	-528	3378	101
10.4	211	1419	40

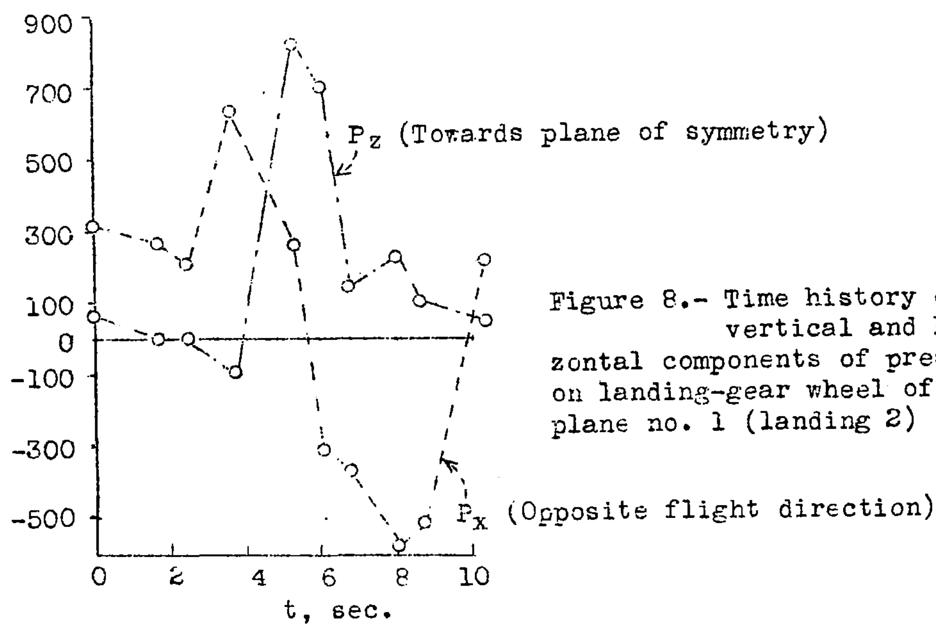

Figure 8.- Time history of vertical and horizontal components of pressure on landing-gear wheel of airplane no. 1 (landing 2)

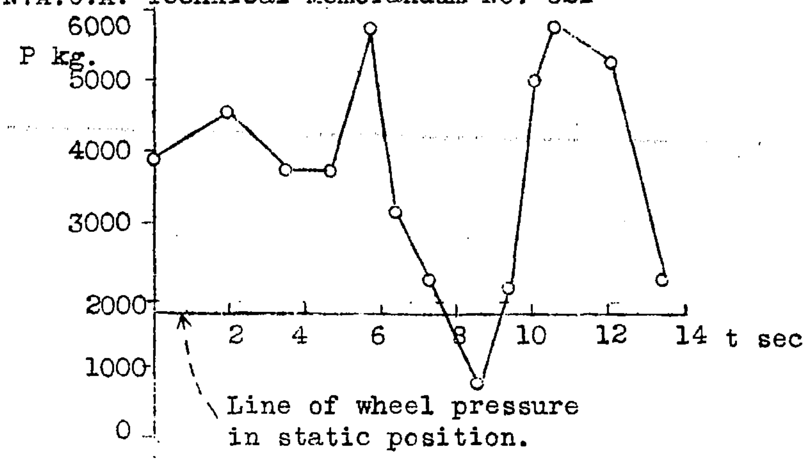

t sec.	P kg.
0	3,867
2	4,529
3.5	3,720
4.72	3,736
5.73	5,690
6.43	3,184
7.3	2,228
8.58	873
9.3	2,061
10	5.024
10.5	5,782
12	5,229
13.4	2,269

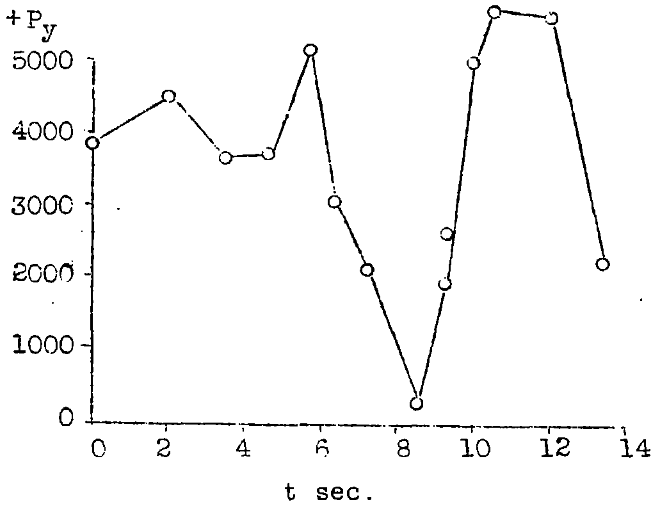

t sec	P_x kg	P_y kg	P_z kg
0	+475	3,833	-203
2	423	4,494	-366
3.5	317	3,690	-355
4.72	211	3,722	-310
5.73	105	5,689	0
6.43	211	3,172	-183
7.3	-475	2,169	-183
8.58	527	404	+567
9.3	527	1,974	+264
10	264	5,013	+204
10.5	527	5,753	-241
12	634	5,183	-285
13.4	212	2,253	-186

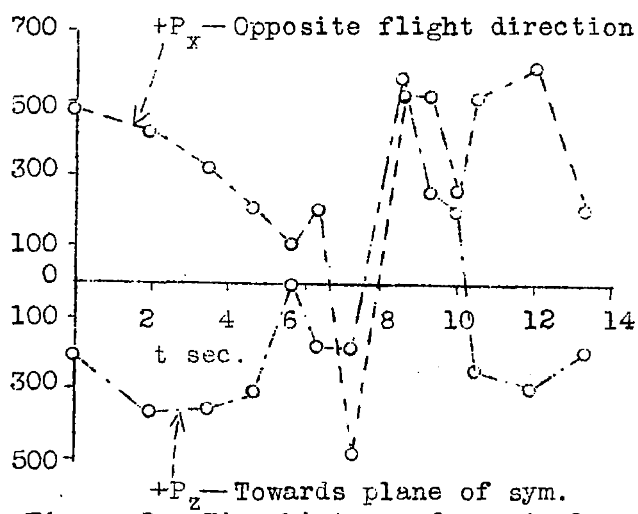

Figure 9.- Time history of vertical and horizontal components of pressure on landing-gear wheel of airplane no. 1 (landing 3).

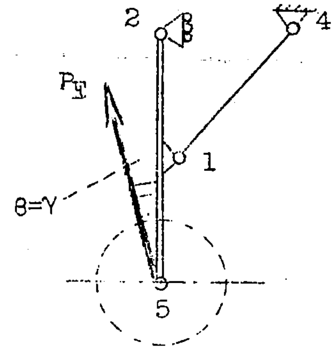

Figure 10.

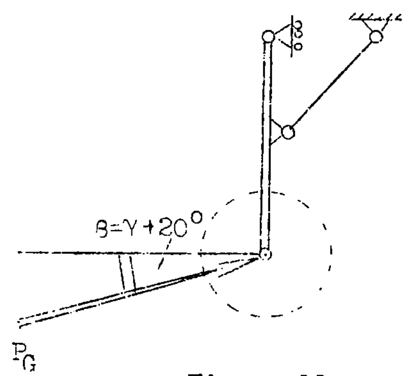

Figure 11.

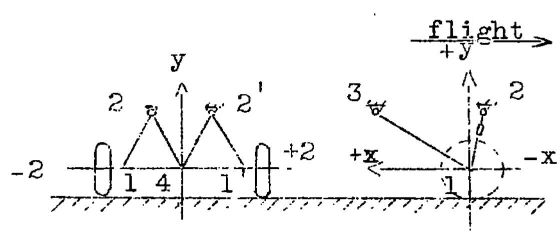

Figure 13.- Landing-gear arrangement of airplane no. 2.

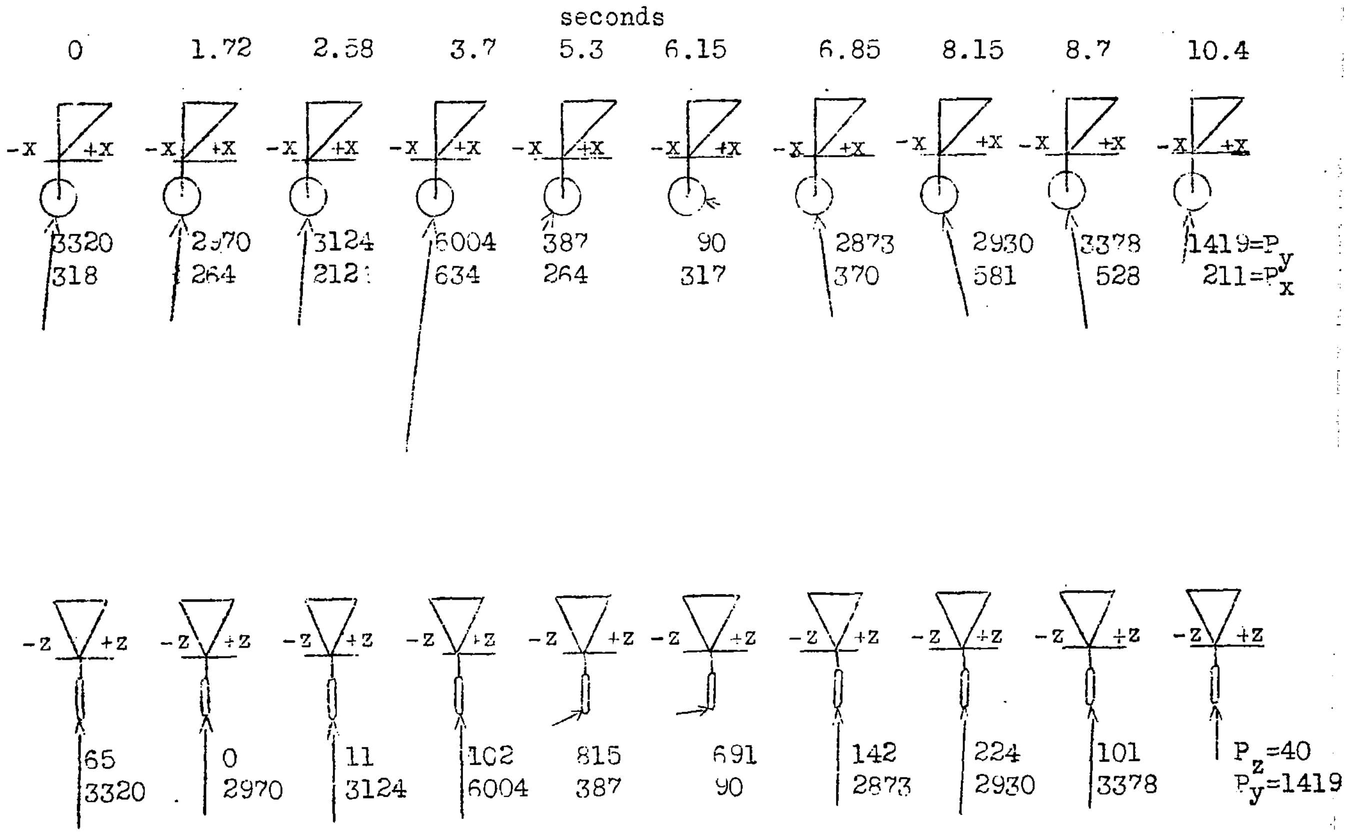

Figure 12.- Time history of forces P_x, P_y and P_z, P_y on landing-gear wheel of airplane no. 1 (landing 2).

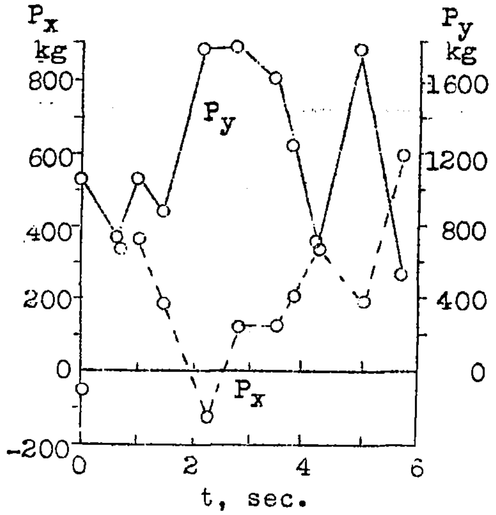

t_{sec}	P_x	P_y
0	- 53	1060
.7	339	708
1.0	358	1060
1.4	194	884
2.2	-123	1773
2.8	123	1773
3.4	123	1595
3.8	210	1240
4.2	339	708
5.0	185	1772
5.7	588	531

Figure 14.- Time history of vertical and horizontal components of pressure on landing-gear wheel of airplane no. 2 (take-off no. 1)

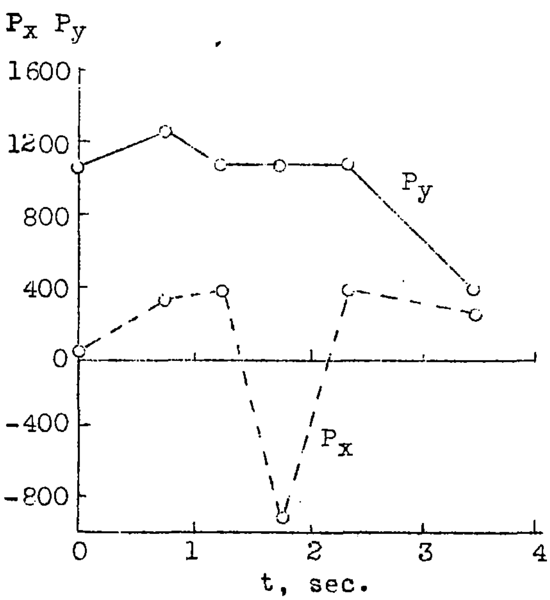

t_{sec}	P_x	P_y
0	50	1064
.76	316	1242
1.26	358	1064
1.76	-874	1064
2.36	353	1064
3.46	222	±359

Figure 15.- Time history of vertical and horizontal components of pressure on landing-gear wheel of airplane no. 2 (take-off no. 2)

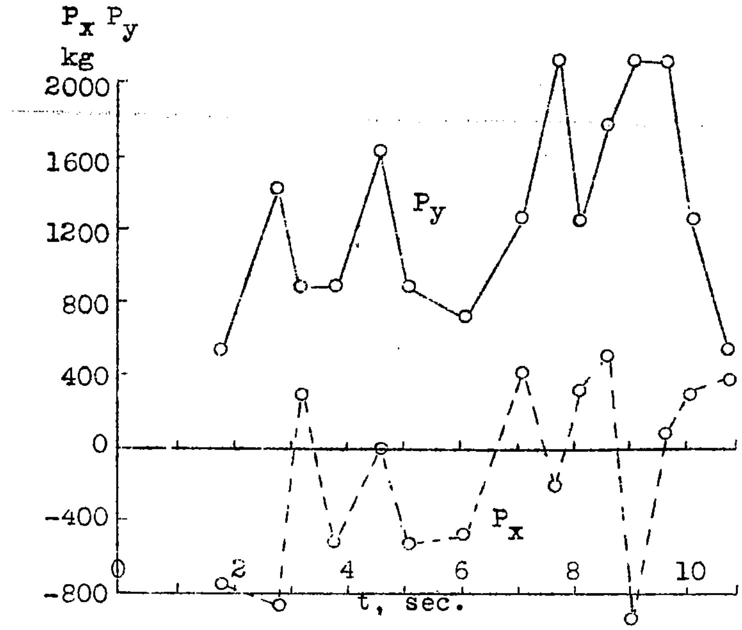

t_{sec}	P_x	P_y
1.8	-746	531
2.8	-857	1420
3.2	296	887
3.8	-524	887
4.6	- 9	1616
5.1	-524	887
6.1	-481	708
7.1	410	1268
7.7	-209	2121
8.1	314	1241
8.6	492	1772
9.1	-928	2121
9.7	99	2121
10.1	314	1241
10.8	383	531

Figure 16.- Time history of vertical and horizontal components of pressure on landing-gear wheel of airplane no. 2 (landing no.1)

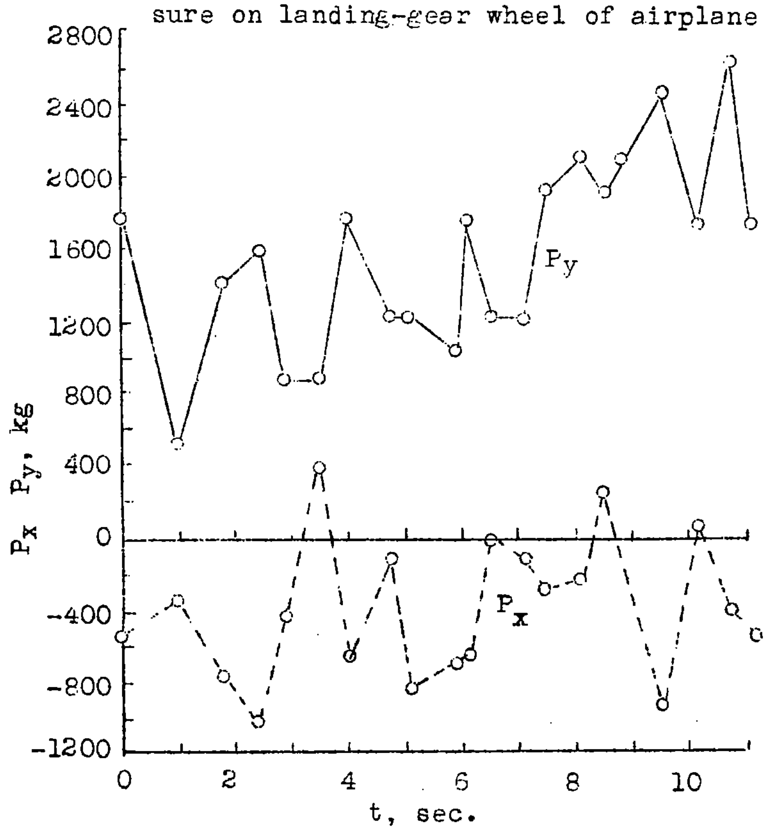

t_{sec}	P_x	P_y
0	- 534	1770
1	- 334	531
1.8	- 750	1415
2.4	-1003	1593
2.9	- 421	885
3.5	399	885
4.0	- 636	1770
4.8	- 97	1240
5.1	- 814	1240
5.9	- 669	1062
6.1	- 636	1770
6.6	5	1240
7.1	- 97	1240
7.5	- 270	1950
8.1	- 210	2123
8.6	270	1950
8.8	- 106	2123
9.6	- 911	2480
10.2	81	1770
10.7	- 385	2659
11.2	- 534	1770

Figure 17.- Time history of vertical and horizontal components of pressure on landing-gear wheel of airplane no.2 (landing no.2)

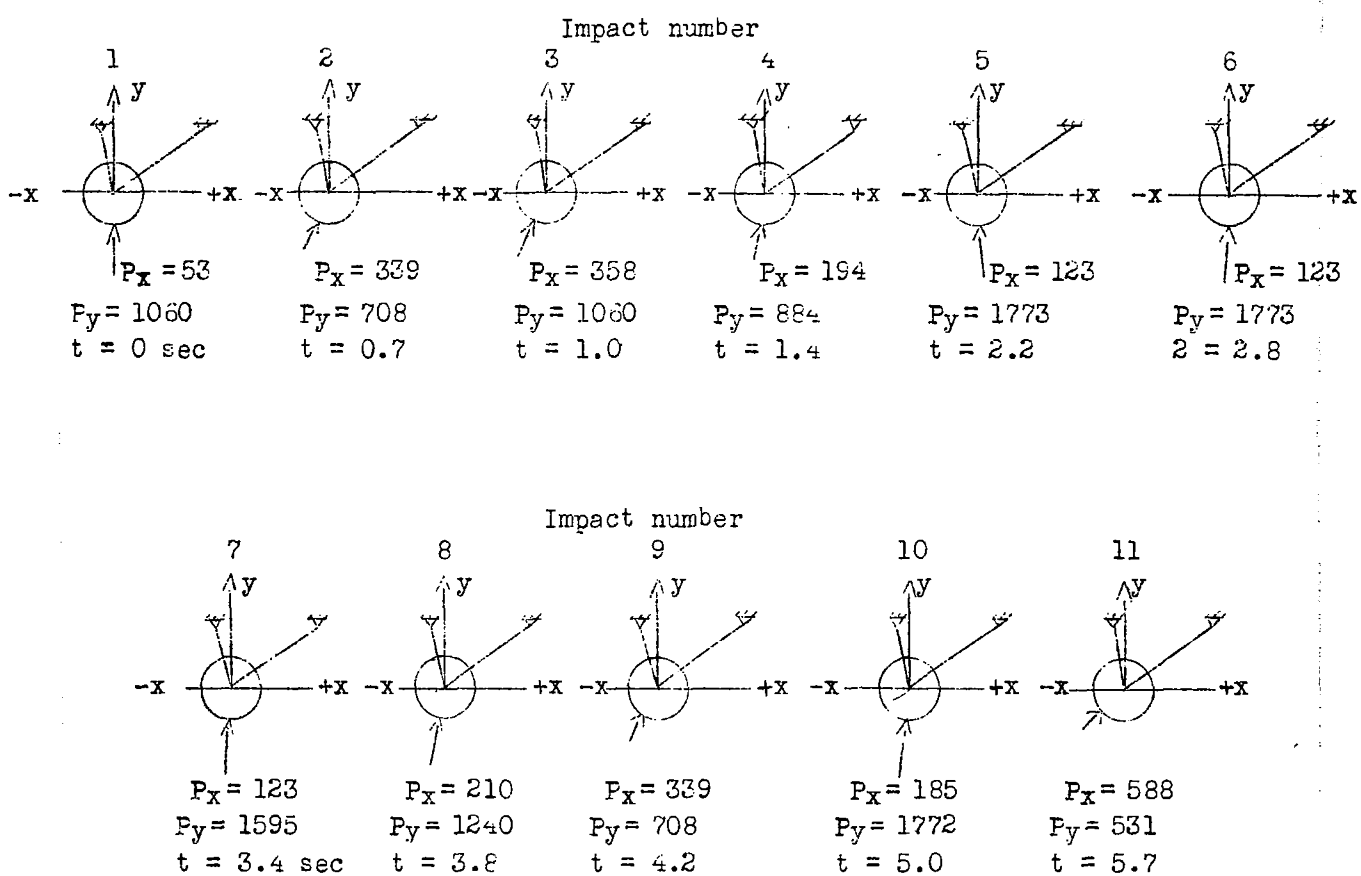

Figure 18.- Time history of external force on landing-gear wheel of airplane no. 2 (take-off 1)